PHYSICAL REVIEW A **81**, 061401(R) (2010)

Vibrationally cold CO^{2+} in intense ultrashort laser pulses

J. McKenna,[1] A. M. Sayler,[1] F. Anis,[1] Nora G. Johnson,[1] B. Gaire,[1] U. Lev,[2] M. A. Zohrabi,[1]
K. D. Carnes,[1] B. D. Esry,[1] and I. Ben-Itzhak[1]

[1]*J. R. Macdonald Laboratory, Department of Physics, Kansas State University, Manhattan, Kansas 66506, USA*

[2]*Department of Particle Physics, Weizmann Institute of Science, Rehovot 76100, Israel*

(Received 19 July 2009; published 3 June 2010)

By virtue of the short lifetime of excited states, we have performed three-dimensional (3D) momentum imaging on the fragments from an electronically and vibrationally cold metastable CO^{2+} beam following irradiation by intense ultrashort laser pulses. This unique target can be described as a two-channel system, since most low-lying electronic states are not accessible by dipole transitions due to their spin state. Laser excitation between the ground $X^3\Pi$ $v=0$ state and the excited $^3\Sigma^-$ state leads to bond softening and above-threshold dissociation, with peaks in kinetic energy release spaced by the photon energy and interesting angular distributions that peak perpendicular to the laser field. These results are compared with our solutions of the 3D time-dependent Schrödinger equation.

DOI: 10.1103/PhysRevA.81.061401 PACS number(s): 33.80.Wz, 42.50.Hz

Intense ultrashort laser pulses are an excellent tool for manipulating molecular dynamics [1]. Consequently there are many applications in physics, chemistry, and biology, for example, in the quest to use lasers to control molecular reactions [2]. Most such applications require a good knowledge of the nonlinear response of a molecule to the laser field. This task is traditionally arduous due to the complexity of most molecular electronic potentials. The challenge is to find ways to simplify the problem to reveal the underlying physics—as we have accomplished in this article.

To limit the level of complexity, studies have tended to focus on the simplest molecule, H_2^+. Studies on H_2^+ are aided by the fact that at low laser intensity its two lowest-lying states $^2\Sigma_g^+$ $(1s\sigma_g)$ and $^2\Sigma_u^+$ $(2p\sigma_u)$ dominate the dissociation as they are energetically isolated from higher excited states. Despite its structural simplicity, even H_2^+ in an intense field is a nontrivial problem as typically its production leads to a broad range of excited $^2\Sigma_g^+$ vibrational states that each respond differently to the laser field. In larger molecules that also involve electronic excitation the difficulty is amplified and has to date hampered the exploration of some well-known processes such as bond softening and above-threshold dissociation [3,4].

As one solution, there has been a lot of interest in vibrational cooling of molecular ions, and several innovative techniques have been proposed [5–9]. Nonetheless, to our knowledge, the only successful intense laser study on cold $v=0$ molecular ions was that recently reported by Orr *et al.* [10]. Those authors stored HD^+ in an electrostatic trapping device [11] long enough (up to 500 ms) for the excited v states to radiatively cool due to the small permanent dipole moment, producing HD^+ in mostly the $^2\Sigma_g^+$ $v=0$ state. That approach, however, was accompanied by difficulties of its own such as low trapping efficiency and large depletion from background collisions due to the long trapping time.

In this article we report on studies of vibrationally cold metastable CO^{2+} ions in intense femtosecond laser pulses. By studying a complex molecule like CO^{2+}, we are able to test the generality of previous knowledge from H_2^+ work. When electronically and vibrationally cold, CO^{2+}, like H_2^+, behaves as a simple two-channel system in an intense laser with its dissociation dynamics governed by the coupling between its ground $X^3\Pi$ and excited $^3\Sigma^-$ states. In contrast to H_2^+, the $\Pi\rightarrow\Sigma$ coupling results in a perpendicular transition dipole-matrix element whereby dissociation tends to result in fragments in the direction orthogonal to the laser polarization. This allows us to explore perpendicular dissociation that so far has been scarcely studied (see [13,14] for some exceptions). We reveal from our measurements the presence of bond softening and above-threshold dissociation peaks in this rather unusual system, in keeping with the common behavior of H_2^+ [4].

By nature, doubly charged diatomic molecules like CO^{2+} are interesting and exotic species. Despite a strong electrostatic repulsion of their nuclei, their unusual bonding properties allow them to overcome these forces and form metastable systems. Dications have been investigated extensively over the years [15], spurred by the important role they play in interstellar and plasma processes. Studies have shown that the lifetimes of dications typically range from picoseconds to many seconds. The CO^{2+} ion is no exception [16].

The lowest-lying potential energy curves of CO^{2+} are shown in Fig. 1(a). By tunneling through the potential barrier and, more importantly, by predissociation along the $^3\Sigma^-$ state mediated by strong spin-orbit coupling, the lifetimes of all states—*except* $X^3\Pi$ $v=0$—have been measured and/or calculated to be less than a microsecond [12,16]. The $X^3\Pi$ $v=0$ is estimated to live between tens of milliseconds and a second. We take advantage of this rapid decay rate of CO^{2+} excited states to produce a beam of electronically and vibrationally cold CO^{2+}.

Carbon monoxide gas is doubly ionized by electron impact in an electron-cyclotron resonance (ECR) ion source. Due to Franck-Condon overlap with the CO ground state, the CO^{2+} ions are populated in a broad range of excited states. They are accelerated to 9 keV, momentum analyzed, and electrostatically focused to form a collimated beam ($\sim$0.6 $\times$ 0.6 mm) that is transported to the laser interaction region. The flight time of 20 μs ensures that all states except the $X^3\Pi$ $v=0$ state have dissociated before reaching the interaction region. This produces a pure target of vibrationally cold $X^3\Pi$ CO^{2+} ions. Laser-induced dissociation fragments, with several keV laboratory energy, are imaged using a coincidence 3D momentum-imaging technique, introduced in an earlier publication [17].

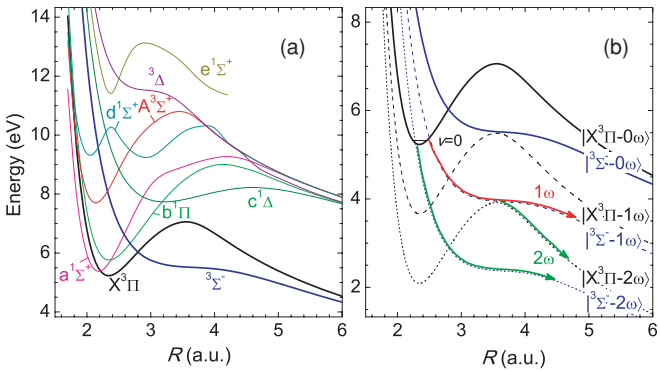

FIG. 1. (Color online) (a) Born-Oppenheimer potentials for CO^{2+} calculated by Šedivcová *et al.* [12]. (b) The diabatic Floquet potentials for the two lowest triplet states. Each curve carries a photon number label. The energy scale is relative to the dissociation limit of $|X^3\Pi - 0\omega\rangle$.

The laser pulses used are from a Ti:sapphire laser (790 nm), with a multipass amplifier, that produces 2-mJ, 40-fs laser pulses at 1-kHz repetition rate. By passing the pulses through a neon-filled hollow core fiber and chirped-mirror arrangement, we compress the pulses to 7 fs when desired. The linearly polarized pulses are focused with an $f = 203$ mm parabolic mirror to a peak intensity in the range of 10^{15} W/cm^2. By moving the overlap of the ion beam away from the center of the laser focus, we sensitively control the interaction intensity. When needed, a β-barium borate crystal is used to produce 395-nm light.

Figures 2(a)–2(g) show kinetic energy release (KER) spectra obtained from dissociation of vibrationally cold $CO^{2+} \rightarrow C^+ + O^+$ by 40 fs [(a)–(c)] and 7 fs [(d)–(g)] pulses at a selection of intensities using 790-nm light. Typical spectra are acquired for ~10 h data-acquisition time each.

For comparison, Fig. 2(h) shows similar coincidence measurements we recorded of $C^+ + O^+$ using 40-fs, 2×10^{15} W/cm^2 pulses but instead for a target of CO gas [18] and a CO^+ ion beam. In these examples, CO^{2+} is produced by ionization of the target with the same laser pulse that is used to dissociate it, which is more traditionally the case (e.g. [19]). The main difference between producing CO^{2+} in this way, and forming it as a cold CO^{2+} ion beam as described here, is that in the laser-produced case, the CO^{2+} is formed electronically and vibrationally hot—it does not have time to predissociate and cool on the femtosecond timescale of the laser interaction. Hence, for the transient, hot CO^{2+} ions, both singlet and triplet electronic states are populated. As a result, singlet and triplet states both contribute to dissociation, convoluting the dynamics and leading to the broad and structured KER distributions observed in Fig. 2(h) and in earlier measurements [19].

The KER spectra for the cold CO^{2+} beam are much less complicated than the spectra for hot CO^{2+} produced by the laser (from CO or CO^+), as is immediately apparent in Figs. 2(a)–2(g). At low intensity, for both 40- and 7-fs pulses, a single KER peak is observed centered at ~6.75 eV with a full-width at half-maximum (FWHM) of ~0.4 eV. This peak is from one-photon (1ω) bond softening dissociation [3]. The pathway leading to dissociation of the $X^3\Pi$ $v = 0$ state is shown in the dressed-states Floquet diagram [20] in Fig. 1(b). The $^3\Sigma^-$ state is "dressed" down by 1ω in the laser field and crosses near the $X^3\Pi$ $v = 0$ state. Near the crossing, $v = 0$ population spills onto $|^3\Sigma^- - 1\omega\rangle$ leading to the asymptotic 1ω dissociation limit. We believe only $|X^3\Pi - 0\omega\rangle$ and $|^3\Sigma^- - 1\omega\rangle$ are involved in dissociation since the triplet $X^3\Pi$ state does not couple efficiently to the singlet states within the laser pulse, and the next dissociative triplet state requires at least four photons to be reached.

From other work on field-free predissociation of CO^{2+}, the KER observed for decay of $X^3\Pi$ $v = 0$ via spin-orbit coupling to $^3\Sigma^-$ is ~5.25 eV [21]. For photodissociation by a 1.57 eV photon, we expect a KER value of ~6.8 eV. The observed value of 6.75 eV is in close agreement with the centroid of the peak from our solution to the 3D time-dependent Schrödinger equation shown as the solid line in Fig. 2(d) (see [22] for our theoretical method; CO^{2+} potential curves and couplings were taken from [12]).

The width of the measured peak in Fig. 2(d), however, is broader (0.4 eV) than indicated by our calculation at 7 fs (0.24 eV), and indeed the agreement is worse at 40 fs since the smaller bandwidth of the photons yields an even narrower peak. There are several possible sources for this broadening

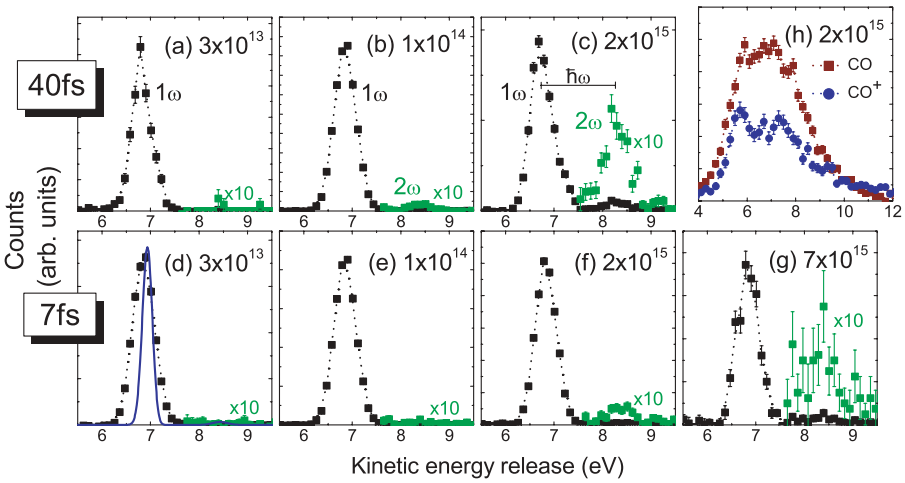

FIG. 2. (Color online) Coincidence dissociation KER spectra of $CO^{2+} \rightarrow C^+ + O^+$ using a target of (a)–(g) vibrationally cold CO^{2+} beam, and (h) CO gas and CO^+ beam. The top row of spectra are using 40-fs pulses and the bottom row 7-fs pulses. Intensities are as indicated in units of W/cm^2. In (a)–(g), the region KER larger than 7.6 eV has been scaled times 10 as indicated to emphasize the ATD 2ω peak. The solid curve in (d) is a calculation (see text) for the same laser conditions as the experiment, but without focal-volume intensity averaging. Error bars denote statistical error.

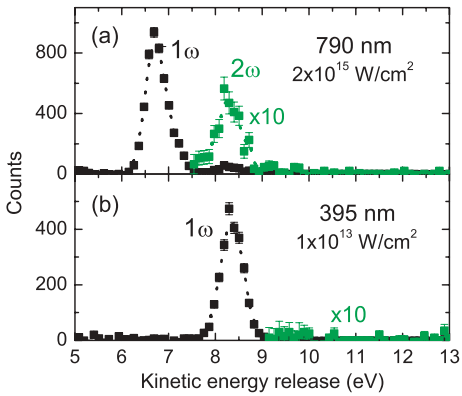

FIG. 3. (Color online) Dissociation KER spectrum using (a) 790-nm, 40-fs pulses at 2×10^{15} W/cm^2 [same as Fig. 2(c)] and (b) 395-nm, 40-fs pulses at 1×10^{13} W/cm^2. Error bars denote statistical error.

in the experiment: (i) We estimate the experimental resolution to be ~0.1 eV at this KER. (ii) Our calculations indicate a broadening of ~0.05 eV from an intensity-dependent Stark shift after laser focal-volume averaging that is not included in the theory curve shown in Fig. 2(d). (iii) Theory shows that the peak width also broadens by ~0.1 eV with decreasing intensity from 3×10^{13} to 10^{11} W/cm^2. (iv) Thermal averaging from the ion source leads to a broadening of up to 0.1 eV. A combination of these and other factors may account for the difference between experiment and theory in Fig. 2(d).

By and large, the trend with intensity follows closely our expectation. At 1×10^{14} W/cm^2, 40 fs, a second peak forms at ~8.3 eV, spaced from the first peak by the photon energy. This is clear evidence of 2ω above-threshold dissociation (ATD) [3] and also shows up in our theory at high intensities. The 2ω peak grows in amplitude for increasing intensity as it becomes more probable for the molecule to absorb the extra photon required. The possible pathways responsible for this peak are shown in Fig. 1(b). There are two ways to reach the 2ω asymptotic limit: (i) by initially coupling from $|X^3\Pi - 0\omega\rangle \rightarrow |^3\Sigma^- - 1\omega\rangle$ at $R = 2.5$ a.u. and then from $|^3\Sigma^- - 1\omega\rangle \rightarrow |X^3\Pi - 2\omega\rangle$ at $R = 3.6$ a.u., or (ii) by directly coupling from $|X^3\Pi - 0\omega\rangle \rightarrow |^3\Sigma^- - 2\omega\rangle$ at $R = 2.3$ a.u.

An indication of the dominant pathway can be determined from comparison of 40 and 7 fs. Pathway (i) requires stretching before reaching the $|^3\Sigma^- - 1\omega\rangle \rightarrow |X^3\Pi - 2\omega\rangle$ crossing. From a classical calculation this requires about 13 fs. Therefore, for a 7-fs pulse there is insufficient time to follow this pathway, suggesting that pathway (ii) must be dominant for 7 fs. In contrast, for 40 fs both pathway (i) and pathway (ii) may occur. Since pathway (i) is a $1\omega + 1\omega$ process it will proceed at lower intensity than a direct 2ω process [23]. Figure 2 confirms that this is the case since the 2ω peak appears at lower intensity for 40 fs indicating the onset of pathway (i) at lower intensity than pathway (ii). This is further attested to by our calculations, which show that the branching ratio of pathway (i) at 40 fs is a factor of ~10 higher than at 7 fs at 1×10^{14} W/cm^2.

To verify the origin of the 8.3 eV peak, we repeated the experiments at 395 nm, 40 fs. We expect the 1ω peak at 395 nm to appear at the same energy as the 2ω peak at 790 nm. Figure 3 shows that this is precisely the case. A single peak is observed for 395 nm [Fig. 3(b)], centered at 8.3 eV with a FWHM of 0.4 eV, similar to the width at 790 nm [Fig. 3(a)]. We further note that at 1×10^{14} W/cm^2 (not shown) no peak is observed near 11.4 eV from 2ω ATD—in spite of ATD being observed at the same intensity using 790 nm. Inspection of the 395-nm dressed-state Floquet picture shows that the $1\omega + 1\omega$ pathway is impossible since the crossing for the second step is absent and, moreover, that the direct 2ω crossing, $|X^3\Pi - 0\omega\rangle \rightarrow |^3\Sigma^- - 2\omega\rangle$, occurs far from the $v = 0$ state, and is thus nonresonant.

It is widely accepted that 1ω dissociation of H_2^+ using short laser pulses leads to a $\sim\cos^2\theta$ angular distribution with respect to the laser polarization $\hat{\varepsilon}$ [24] as we have measured in Fig. 4(a). The $\cos^2\theta$ distribution arises as a result of a parallel transition between the lowest electronic states of H_2^+ (i.e., $^2\Sigma_g^+ \rightarrow {}^2\Sigma_u^+$). The broad initial ro-vibrational states distribution of H_2^+, however, makes it difficult to study single-state behavior and complicates the detailed interpretation generally. In this respect, vibrationally cold CO^{2+} is a more favorable candidate.

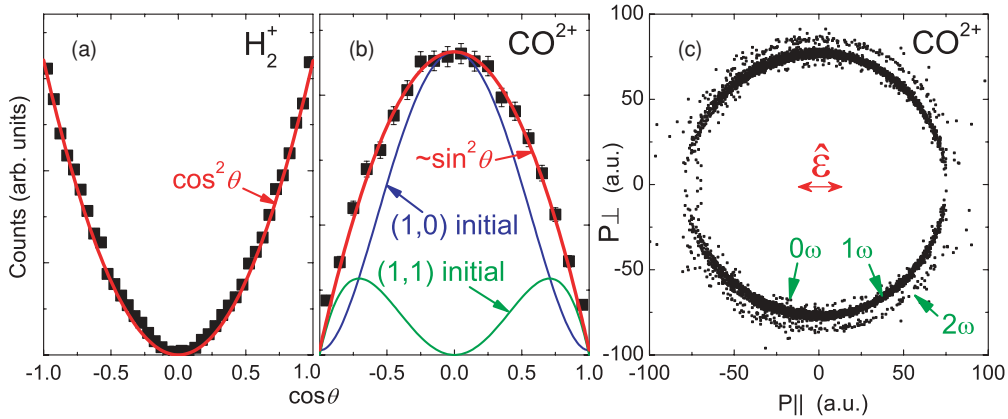

FIG. 4. (Color online) (a) and (b) Angular distribution for 1ω dissociation of (a) H_2^+ (for KER between 0.74 eV and 0.88 eV corresponding to the 1ω crossing), and (b) CO^{2+}, using 40-fs, 1×10^{14} W/cm^2 pulses. The data points are the experiment while the solid lines in (b) are from first-order perturbation theory; see text. (c) Momentum plot for CO^{2+} at 40 fs, 2×10^{15} W/cm^2.

One-photon dissociation occurs by a perpendicular transition between the CO^{2+} $X^3\Pi$ and $^3\Sigma^-$ states, and the leading order angular distribution can be obtained from first-order time-dependent perturbation theory. More specifically, we assume CO^{2+} $X^3\Pi$ is statistically populated initially with one-third $(J,M)=(1,0)$ and two-thirds (1,1), where J and M are the total orbital angular momentum and its projection, respectively. One-photon excitation to $^3\Sigma^-$ leads to a linear combination of (0,0) and (2,0) when starting from (1,0), and to (2,1) when starting from (1,1). The resulting perturbation theory angular distributions for each of these initial (J,M) states are shown in Fig. 4(b) along with their sum and the experimental results. So, even though the individual (J,M) contributions do not yield the expected $\sim\sin^2\theta$ distribution, their sum remarkably does—in good agreement with experiment.

To emphasize this predominantly perpendicular breakup of CO^{2+} we plot the dissociation momentum parallel ($P_\parallel$) and perpendicular ($P_\perp$) to $\hat{\varepsilon}$ in Fig. 4(c). Two rings from 1ω and 2ω dissociation are clearly visible, both peaked perpendicular to $\hat{\varepsilon}$. In fact, hints of a weak third inner ring are also visible, centered with KER 5.3 eV. After ruling out predissociation as a possible cause, we assign this feature to laser-induced below-threshold 0ω dissociation [25] along $|^3\Sigma^- - 0\omega\rangle$ [Fig. 1(b)]. This channel is exciting as it shows directly how the laser distorts the CO^{2+} bond. More detailed measurements are required to investigate it further.

The efficiency with which we have been able to produce a cold beam of CO^{2+} has benefited from the short lifetime of the CO^{2+} excited states. In this respect, there is a large family of dications with comparable properties to CO^{2+}. Studies on these molecules would enable further tests of the role of vibrational and electronic excitation in dissociation. Additionally, as an extension to the present work one could employ a pump and probe scheme on CO to explore the time evolution of the decay of the CO^{2+} short-lived states—thereby learning about, and potentially controlling, the tunneling and/or predissociation processes. Attosecond XUV pulses [26] are available to excite the system with exceptional time resolution and to selectively populate states within a chosen energy range.

In closing, we have successfully measured the intense-field dissociation of an electronically and vibrationally cold molecular ion beam, and in doing so, uniquely identified the fragmentation channels and accessed the related physics. Despite the additional complexity, we find that CO^{2+} in its $X^3\Pi$ ($v=0$) ground state can be described using similar language and concepts that were developed for H_2^+. Dissociation is dominated by bond softening while above-threshold dissociation is evidenced by photon-energy separated peaks. This molecule has also allowed us to cleanly study the coupling between Π and Σ states leading to a perpendicular angular distribution.

ACKNOWLEDGMENTS

We thank Dr. Šedivcová-Uhlikova and Prof. Špirko for communicating their potential energy curves and the couplings of CO^{2+}. We also thank Prof. Z. Chang and his group members, and Dr. C. W. Fehrenbach and Prof. W. Wolff for assistance with the laser and ion beams, respectively. This work was supported by the Chemical Sciences, Geosciences, and Biosciences Division, Office of Basic Energy Sciences, Office of Science, US Department of Energy.

[1] J. H. Posthumus, Rep. Prog. Phys. **67**, 623 (2004).
[2] M. F. Kling *et al.*, Science **312**, 246 (2006).
[3] A. Giusti-Suzor, X. He, O. Atabek, and F. H. Mies, Phys. Rev. Lett. **64**, 515 (1990).
[4] P. H. Bucksbaum, A. Zavriyev, H. G. Muller, and D. W. Schumacher, Phys. Rev. Lett. **64**, 1883 (1990).
[5] H. Niikura, D. M. Villeneuve, and P. B. Corkum, Phys. Rev. Lett. **92**, 133002 (2004).
[6] D. S. Murphy *et al.*, New J. Phys. **9**, 260 (2007).
[7] T. Niederhausen and U. Thumm, Phys. Rev. A **77**, 013407 (2008).
[8] X. Urbain *et al.*, Phys. Rev. Lett. **92**, 163004 (2004).
[9] T. K. Kjeldsen and L. B. Madsen, Phys. Rev. Lett. **95**, 073004 (2005).
[10] P. A. Orr *et al.*, Phys. Rev. Lett. **98**, 163001 (2007).
[11] D. Zajfman *et al.*, Phys. Rev. A **55**, R1577 (1997).
[12] T. Šedivcová *et al.*, J. Chem. Phys. **124**, 214303 (2006).
[13] A. Talebpour, K. Vijayalakshmi, A. D. Bandrauk, T. T. Nguyen-Dang, and S. L. Chin, Phys. Rev. A **62**, 042708 (2000).
[14] K. Vijayalakshmi *et al.*, Phys. Rev. A **62**, 053408 (2000).
[15] D. Mathur, Phys. Rep. **391**, 1 (2004).
[16] J. P. Bouhnik *et al.*, Phys. Rev. A **63**, 032509 (2001).
[17] I. Ben-Itzhak *et al.*, Phys. Rev. Lett. **95**, 073002 (2005).
[18] We used a Wiley-McLaren time-of-flight spectrometer with CO gas, recording C^+ and O^+ in coincidence.
[19] D. L. Hatten *et al.*, Las. Phys. **7**, 858 (1997).
[20] S. I. Chu and D. Telnov, Phys. Rep. **390**, 1 (2004).
[21] M. Lundqvist, P. Baltzer, D. Edvardsson, L. Karlsson, and B. Wannberg, Phys. Rev. Lett. **75**, 1058 (1995).
[22] F. Anis and B. D. Esry, Phys. Rev. A **77**, 033416 (2008).
[23] A. M. Sayler, P. Q. Wang, K. D. Carnes, B. D. Esry, and I. Ben-Itzhak, Phys. Rev. A **75**, 063420 (2007).
[24] K. Sändig, H. Figger, and T. W. Hänsch, Phys. Rev. Lett. **85**, 4876 (2000).
[25] J. H. Posthumus *et al.*, J. Phys. B **33**, L563 (2000).
[26] G. Sansone *et al.*, Science **314**, 443 (2006).